Mathematics in Engineering, 5(4): 1–13.
DOI:10.3934/mine.2023076
Received: 18 November 2022
Revised: 05 February 2023
Accepted: 05 February 2023
Published: 17 February 2023

http://www.aimspress.com/journal/mine

Research article

Fibonacci signals with timing jitter

D. S. Citrin[1,2,*]

[1] School of Electrical and Computer Engineering, Georgia Institute of Technology, Atlanta, Georgia 30332-0250, USA

[2] Georgia Tech-CNRS IRL 2958, Georgia Tech Europe, 2 Rue Marconi, 57070 Metz, France

* **Correspondence:** Email: david.citrin@ece.gatech.edu.

Abstract: The power spectral density of a signal comprised of a sequence of Dirac δ-functions at successive times determined by a Fibonacci sequence is the temporal analog of the well known structure factor for a Fibonacci chain. Such a signal is quasi-periodic and, under suitable choice of parameters, is the temporal analog of a one-dimensional quasicrystal. While the effects of disorder in the spatial case of Fibonacci chains has been studied numerically, having an analytically tractable stochastic model is needed both for the spatial and temporal cases to be able to study these effects as model parameters are varied. Here, we consider the effects of errors in where the δ-functions defining the signal in the temporal case occur, i.e., timing jitter. In this work, we present an analytically tractable theory of how timing jitter affects the power spectral density of Fibonacci signals.

Keywords: Fibonacci sequences; nonperiodic sampling; timing jitter

1. Introduction

Fibonacci chains are quasiperiodic one-dimensional systems whose structural or material properties follow a Fibonacci sequence [1–3]. Fibonacci multilayered structures have been realized that exhibit structural [4, 5], electronic [1, 2, 6–12], acoustic [13–15], diffusive [16], plasmonic [17, 18], electrical [19–21], and electromagentic [22, 23] properties. Historically, of particular interest are Fibonacci superlattices which are epitaxially grown multilayered semiconductor structures where the sequence of semiconductor layer thicknesses follows a Fibonacci sequence [3]. Such quasi-periodic structures for suitable choice of the parameters realize one-dimensional quasicrystals [24]. Unlike periodic systems, Fibonacci systems possess two incommensurate periods, and are thus called quasiperiodic. Fibonacci superlattices were extensively studied in the 1980's as they were a relatively straightforward way to realize an artificial one-dimensional quasicrystal. Spectral properties of Fibonacci chains are thoroughly reviewed in [25–27]. Quasi-crystal Fibonacci chains have their two incommensurate

periods in the golden ratio $\phi = (1 + \sqrt{5})/2$. The static structure factor (structure factor by default) of Fibonacci chains is broadband consisting of many sharp peaks; in the limit the chain is of infinite length, these tend to Dirac δ-functions giving rise to a singluar-continuous spectrum. Specifically, the set of wavevectors corresponding to peaks in the structure factor is dense in the sense that for any wavevector, there is a peak arbitrarily close to it. A Fibonacci chain exhibits a characteristic structure factor in some senses intermediate between the periodic or random cases. In the case of Fibonacci superlattice, perhaps the most thoroughly studied physical realization of the concept of a Fibonacci chain, epitaxial structures suffer from errors in the layer thicknesses as well as interface roughness; however, the basic spectral properties of real Fibonacci superlattices were found to be reasonably robust against such uncertainties in layer thicknesses in the sense that the main spectroscopic signatures of the underlying Fibonacci structure persist even in the presence of modest disorder.

The foregoing discussion concerns Fibonacci chains, but Fibonacci temporal sequences should also be explored for *temporal* signals as well. The spectroscopic properties may be attractive for some applications. For example, Ref. [28] suggests cryptographic keys (in the context of spatial Fibonacci chains). Fibonacci signals are of interest due to their simultaneous broadband nature coupled with the appearance in the power spectral density (PSD) $S_0(\omega)$ of numerous narrow lines. The spectra may be regarded for practical applications as quasi-random, despite the fact that they arise from a deterministic process. Applications in broadband radar and communications as well as cryptography may suggest themselves.

In view of possible applications, the effects of timing jitter $\xi(t)$, which will slightly vary the temporal occurences of the Dirac-δ functions comprising the Fibonacci signal, is germane. To gain insight into this problem, we turn to the literature related to disorder in Fibonacci chains and superlattices. Ref. [4] carried out X-ray diffraction on a Fibonacci superlattice and found that despite a roughly 5% error in the thicknesses of the layers, the diffractogram exhibited the expected pronounced peaks; Ref. [29] carried out theoretical studies of the effects of disorder on a Fibonacci chain. As the type of disorder present in superlattices has nothing directly to do with *Fibonacci* superlattices, we can look to the literature on periodic superlattices. Though the literature is extensive, a key study is Ref. [30] where a disorder model similar in some ways to one in which long-time order is not preserved was found to apply to the experimental x-ray diffraction data for the superlattice studied, though the model really requires one to understand the superlattice structure in three dimensions. For the Fibonacci signal, however, such complications are not required.

In the first disorder model explored in both Refs. [4] and [29] the on-site energies in a nearest-neighbor tight-binding model (which we can regard as a surrogate for layer thickness variations) are uniformly distributed around a symmetric interval about the nominal (i.e., mean) site energies. They found that the resulting spectrum was remarkably unaffected by the fluctuations up to a few percent. That is, for the finite-length Fibonacci chains studied, the peaks in the structure factor persisted in the presence of this disorder type in which long-range order is preserved. This disorder model is analogous to one of the timing-jitter models we consider below, in which there is a clock that is locked to an oscillator keeping absolute time. Timing jitter is thus around the absolute time. We also find that all the peaks, in the PSD $S_0(\omega)$ in the absence of timing jitter $\xi(t)$ also appear in $S(\omega)$ in the presence of timing jitter; $S_0(\omega)$ denotes the PSD in the absence of jitter, while $S(\omega)$ with jitter. (We also find additional features, the appearance of pedestals under the peaks; see below.) We also consider a second timing-jitter model in which the clock is a self-sustaining oscillator [31]. In this case, the

nominal timing wanders from the absolute time and the peaks are broadened and merge.

In this study, we consider the spectral properties of Fibonacci signals in the presence of timing jitter $\xi(t)$. In particular, we compute the PSD $S(\omega)$ of such signals. That is, we explore the effects of $\xi(t)$ on $S(\omega)$. Timing jitter that does not preserve-long-time order not only tends to broaden peaks in $S(\omega)$, but actually is found to suppress important quasiperiodic properties of a Fibonacci signal; timing jitter that preserves long-time order results in a PSD in which all peaks in $S_0(\omega)$ continue to be present. To carry out our study, we consider generic timing-jitter models that were developed to capture basic effects on the PSD of oscillators. The type that destroys long-time order is associated with a clock constituted by what Lax calls a *self-sustained oscillator* [31]. In this case, the timing jitter associated with the clock can wander with no effective restoring force. The second type of timing jitter which preserves long-time order is described by an Adler-type system [32] in which the clock oscillator is locked to the true time scale so that there is effectively a restoring force maintaining the oscillator close to the true time. This model was adapted by Haus [33] to mode-locking of lasers. In fact, the two models can be employed in combination as we do below. While these models are to some degree generic, they have proven successful in describing the main effects of timing jitter and can be used to illustrate the contrasting effects of these two types of timing jitter. The models clearly leave out much of the physics of the noise generation and how the fundamental noise that leads to timing jitter propagates through the system. That is, the fundamental noise may be subject to system-specific filtering–linear and nonlinear–as well as time delays of particular import in systems with time-delay feedback [34]. These effects are not included here.

2. Approach

Let us begin by pointing out the basic quantity, the structure factor, in the spatial case. The PSD will be entirely analogous. A key quantity with regard to a *spatial* Fibonacci chain is the structure factor [35],

$$S(q) = \frac{1}{n+1} \sum_{k,k'=0}^{n} e^{iq(z_k - z_{k'})} \tag{2.1}$$

where q is the wavevector, n is the number of sites in an Nth generation Fibonacci chain, and z_k is the position of the kth lattice site. Here we assume the scattering strength of each lattice site is the same and normalize $S(\omega)$ to facilitate the comparison for different generation N.

Our focus is on Fibonacci *signals*, the direct temporal analog of a Fibonacci chain. Basically, we change z_k to t_k (the time of the kth δ-function impulse in the signal) and q to (angular) frequency ω (the angular frequency). We begin with the signal

$$f(t) = \sum_{k=0}^{N} \delta[t - t_k - \xi(t)] \tag{2.2}$$

where t_k are the times given by an Nth-generation Fibonacci temporal sequence (see below for explicit expressions) and $\xi(t)$ is timing jitter, i.e., error in the clock. We assume that $\xi(t)$ is generated by a zero-mean stationary random process with $\langle \xi(t) \rangle = 0$ and $\langle \xi(t)\xi(t) \rangle = \sigma^2$ with σ the standard deviation of $\xi(t)$. We also assume the process is ergotic, so that we may evaluate time averages as configuration averages. We denote by $f_0(t)$ the signal in the absence of timing jitter. Note that $f(t)$ is a finite-duration signal.

The power spectral density (PSD) of this signal is the temporal analog of the dynamic structure factor. It is

$$S(\omega) = \frac{1}{n+1} \int_{-\infty}^{\infty} dt \int_{-\infty}^{\infty} dt' \, e^{i\omega(t-t')} \langle f(t) f(t') \rangle \tag{2.3}$$

where $\langle \cdots \rangle$ is the time average of the quantity contained within. The PSD can equally be viewed as the squared modulus of the Fourier transform of $f(t)$ averaged over the timing jitter or as the Fourier transform of the autocorrelation function of $f(t)$. If the timescale over which $\xi(t)$ varies is much longer than the duration between successive t_k's, that is, if the instances where $\xi(t_k)$ is so large that, say, $t_k + \xi(t_k) > t_{k+1} + \xi(t_{k+1})$ is so rare that we can neglect such instances, then we can take

$$f(t) = \sum_{k=0}^{N} \delta[t - t_k - \xi(t_k)] \tag{2.4}$$

and

$$S(\omega) = \frac{1}{n+1} \sum_{k,k'=0}^{n} e^{i\omega(t_k - t_{k'})} \langle e^{i\omega \Xi(t_k - t_{k'})} \rangle \tag{2.5}$$

where $\Xi(t_k - t_{k'}) = \xi(t_k) - \xi(t_{k'})$ and we use the fact that for a stationary random process, $\Xi(t_k - t_{k'})$ only depends on $|t_k - t_{k'}|$. The frequency ω arises naturally in the exponent. Its physical meaning is that for a given timing jitter $\xi(t)$, the *phase noise* for a sinusoid at frequency ω is $\omega\xi(t)$. Although exact expressions exist for $S_0(\omega)$ [5], we shall need the expression of Eq (2.5) when we include the effects of $\xi(t)$. Below, we evaluate the time-averaged quantity in Eq (2.5) for the two types of timing jitter.

Before we do so, we consider a Fibonacci sequence that determines the time difference $t_{k+1} - t_k$ in an Nth generation Fibonacci sequence seeded by the two time durations τ_A and τ_B. Define the rule

$$F_N = F_{N-1} \otimes F_{N-2} \tag{2.6}$$

giving the sequence F_N of τ_A's and τ_B's of the Nth generation. Thus, for the first few generations, we have the sequences of τ_A's and τ_B's,

$$\begin{aligned}
F_1 &= \tau_A, \\
F_2 &= \tau_A \, \tau_B, \\
F_3 &= \tau_A \, \tau_B \, \tau_A, \\
F_4 &= \tau_A \, \tau_B \, \tau_A \, \tau_A \, \tau_B, \\
F_5 &= \tau_A \, \tau_B \, \tau_A \, \tau_A \, \tau_B \, \tau_A \, \tau_B \, \tau_A.
\end{aligned}$$

As for the values of t_k, we have

$$\begin{aligned}
t_0 &= 0, \\
t_1 &= \tau_A, \\
t_2 &= \tau_A + \tau_B, \\
t_3 &= \tau_A + \tau_B + \tau_A, \\
t_4 &= \tau_A + \tau_B + \tau_A + \tau_A + \tau_B, \\
t_5 &= \tau_A + \tau_B + \tau_A + \tau_A + \tau_B + \tau_A + \tau_B + \tau_A,
\end{aligned}$$

etc., up to t_N for the Nth generation Fibonacci sequence.

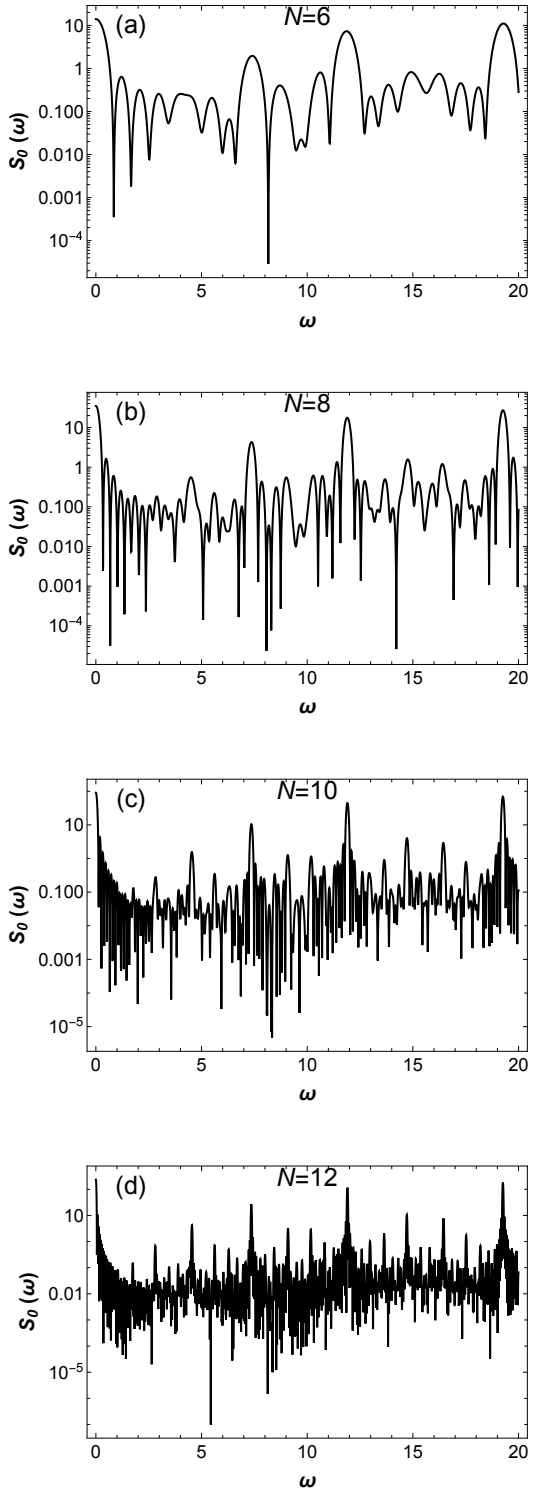

Figure 1. $S_0(\omega)$ for (a) $N = 6$, (b) 8, (c) 10, and (d) 12 generation Fibonacci signals in the absence of timing jitter $\xi(t)$. The main peaks are at $\omega = 2\pi\phi^p/\tau_F$ with $p \in \mathbb{W}$ and $\tau_F = \phi\tau_A + \tau_B$.

We consider $\tau_A = \phi/(1+\phi)$ and $\tau_B = 1/(1+\phi)$. We have for convenience chosen these values such that $\tau_A + \tau_B = 1$ (without loss of generality) and $\tau_A/\tau_B = \phi$ (see below) giving a signal that is a time-analogue of a one-dimensional quasicrystal. Figure 1 shows the PSD $S_0(\omega)$ in the absence of timing jitter for an (a) $N = 6$, (b) 8, (c) 10, and (d) 12 generation Fibonacci signal. As N increases, the number of peaks in the PSD increases while the linewidths decrease. These lineshapes, even in the absence of timing jitter, are Lorentzian with the width decreasing with increasing generation N. The peaks at small ω for modest N mainly reflect the finite thickness of the Nth generation Fibonacci signal. In the limit $N \to \infty$, the peaks are δ-functions, and in general for Fibonacci signals occur when $\omega = 2\pi(m+n\phi)/\tau_F$ where $\tau_F = (\phi t_A + \tau_B)$. The largest peaks occur when $0 \approx \pi\tau^2(m\tau_A - n\tau_B)$ with $m, n \in \mathbb{Z}$. For $\tau_A/\tau_B = \phi$, the main peaks are at $\omega = 2\pi\phi^p/\tau_F$ with $p \in \mathbb{W}$ and in this case $\tau_F = \phi\tau_A + \tau_B$. The large peaks for the first few p are evident in all panels of Figure 1, which shows $S_0(\omega)$ for (a) $N = 6$, (b) 8, (c) 10, and (d) 12. These plots reproduce well known features of the structure factor (but here in the PSD in the frequency rather than the wavevector domain) of Fibonacci chains [25, 26].

We next turn to the case in which timing jitter $\xi(t)$ is present. We have the expression of Eq (2.5) for $S(\omega)$, which is the Wiener-Khinchine spectrum [36, 37]. We adopt a combined model for the timing jitter, as mentioned above, that accounts for clock wander and for a locking oscillator. Since the model is discussed in detail in Refs. [31, 33, 38], we refer the reader to those works. Note also as mentioned above, we assume the fundamental noise is unfiltered by the system. In short, the characteristic function encountered above is

$$\langle e^{i\omega\Xi(t_k - t_{k'})}\rangle = e^{-\Lambda\omega|t_k - t_{k'}|}\exp[-\omega^2\sigma^2(1 - e^{-2|t_k - t_{k'}|/\tilde{\tau}})]. \tag{2.7}$$

Here, Λ is the rate at which the phase at frequency ω wanders from the value it would have determined by an absolute clock and $\tilde{\tau}$ is the correlation time of the locking oscillator. σ, recall, is the standard deviation of the timing jitter of the locking oscillator. Note that inherent in these models is timing jitter that is Gaussian at all times but where time-correlations nonetheless can lead to Lorentzian lineshapes in the PSD. Of course one can imaging physical systems in which the timing jitter is distributed differently or with different temporal correlations; however, this model has proven to be quite successful for a range of physical oscillators. It also enables the clear distinction of timing jitter that preserves or destroys long-time order and has the benefit of enabling analytically tractable results for a stochastic model.

For the case without the presence of the locking oscillator, the timing jitter $\xi(t)$ obeys a one-dimensional diffusion equation [31]. The timing thus can wander since there is no restoring force maintaining t_k near its nominal value. Ref. [31] considers the phase noise of an otherwise monochromatic oscillator, and thus the phase noise associated with the timing jitter $\xi(t)$ on an oscillator of frequency ω is $\omega\xi(t)$. In the case of a locking oscillator [33], $\varepsilon(t)$ may not wander far from the correct value; in effect, $\xi(t)$ approximately obeys a one-dimensional diffusion equation in a harmonic potential [38], thus providing a restoring force preventing t_k from departing strongly from its nominal value. Our timing-jitter model allows for both effects [38].

3. Results

In the following, we explore the effects of $\xi(t)$ on $S(\omega)$. For clarity, we consider the two types of timing jitter separately, though using Eq (2.7) both can be accounted for simultaneously. Specifically,

we consider two cases: first the effects of Λ with $\sigma = 0$ (self-sustaining oscillator) and second the effects of σ and $\tilde{\tau}$ with $\Lambda = 0$ (locking oscillator). In Figures 2 and 3 are plotted $S(\omega)$ for $N = 8$ (Figure 2) and 12 (Figure 3) for (a) $\Lambda = 0.01$ and (b) 0.1 with $\sigma = 0$. We choose $N = 8$ and 12 to make the main effects clear, and also to compare with published work on Fibonacci superlattices, which for practical reasons are limited to modest $N \sim 10$. We see that for increasing Λ, while the most dominant peaks persist, they are increasingly broadened, an effect that becomes more severe with increasing ω. At the same time, the plethora of small, narrow peaks in Figure 1(b) and (d) are no longer visually evident. The merging of the broadened peaks as ω increases lead to an apparent featureless floor above which the residues of the main peaks rise. Comparing Figures 2(b) and 3(b), for large Λ the PSD is similar for both values of N as the finite-N-induced broadening has been dominated by broadening associated with Λ. That is, Λ limits the temporal range over which the signal remains coherent.

Figures 4 and 5 show $S(\omega)$ for $N = 8$ (Figure 4) and 12 (Figure 5) for (a) $\sigma = 0.01$ and (b) 0.1 both with $\tilde{\tau} = 10$ and $\Lambda = 0$. Here the effect of $\xi(t)$ is markedly different. That is, the correlation time $\tilde{\tau}$ is over ~ 10 pulses. Focusing on Figure 5, where the effect is more evident (the peaks are already fairly broad in Figure 4 simply due to the generation number $N = 8$; see Figure 1(b)), timing jitter associated with a locking oscillator does not blur the various spectral lines, but instead introduces a pedestal upon which each peak sits. The contribution of the pedestals increases with ω; the peaks themselves remain sharp on top of the pedestals. That is, the associated timing jitter still leaves a long-term coherence.

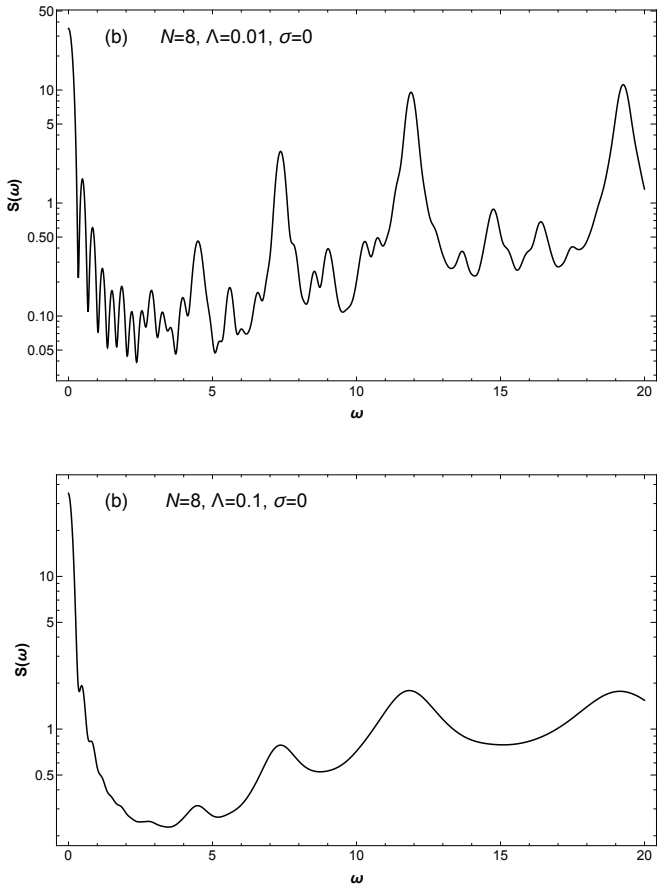

Figure 2. $S(\omega)$ for $N = 8$ for (a) $\Lambda = 0.01$ and (b) 0.1 with $\sigma = 0$.

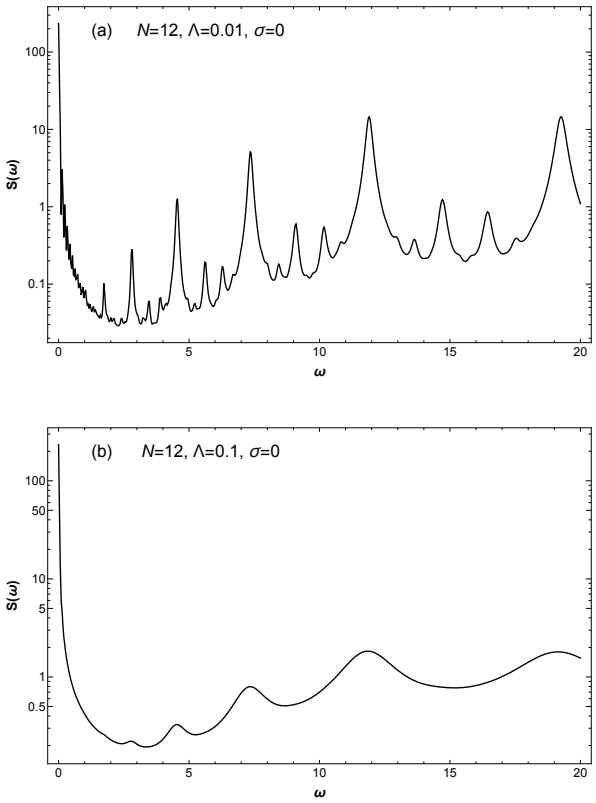

Figure 3. $S(\omega)$ for $N = 12$ for (a) $\Lambda = 0.01$ and (b) 0.1 with $\sigma = 0$.

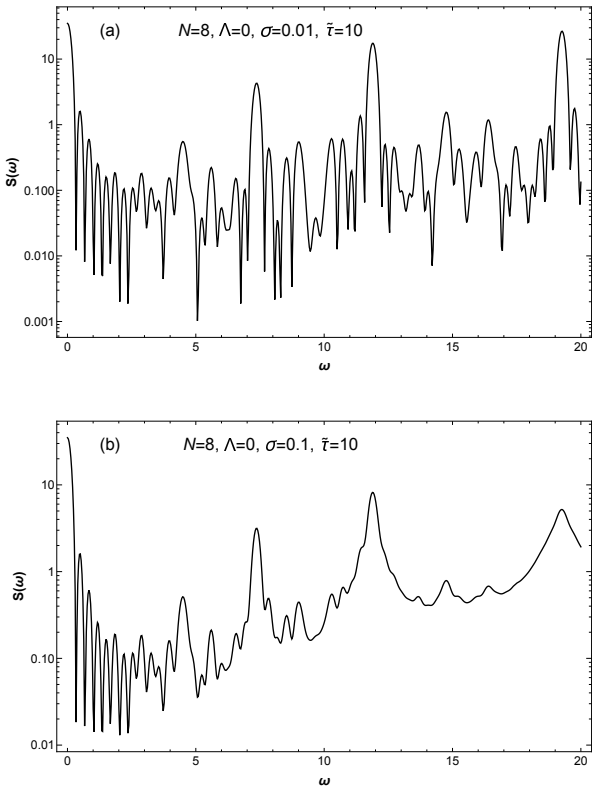

Figure 4. $S(\omega)$ for $N = 8$ for (a) $\sigma = 0.01$ and (b) 0.1 with $\Lambda = 0$ and $\tilde{\tau} = 10$.

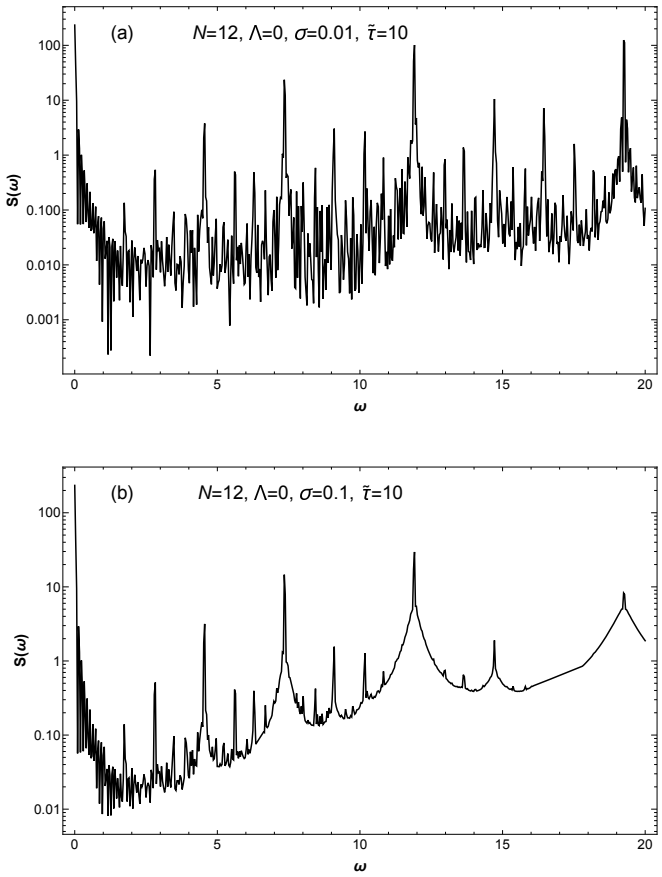

Figure 5. $S(\omega)$ for $N = 12$ for (a) $\sigma = 0.01$ and (b) 0.1 with $\Lambda = 0$ and $\tilde{\tau} = 10$.

Now consider reducing the coherence time, so that $\tilde{\tau} = 5$ with $\sigma = 0.1$ and $\Lambda = 0$ in Figure 6 for $N = 12$. Still, the sharp peaks at line center persist, though the relative weight in the pedestals increases and the pedestals broaden. These types of effects were observed in [33,38], which considered the effects of timing jitter on mode-locked lasers. Easily verified, but not shown, in the $\tilde{\tau} \to 0$ limit, the pedestals merge to form a featureless continuum that rises with ω on which the unbroadened peaks of $S_0(\omega)$ sit.

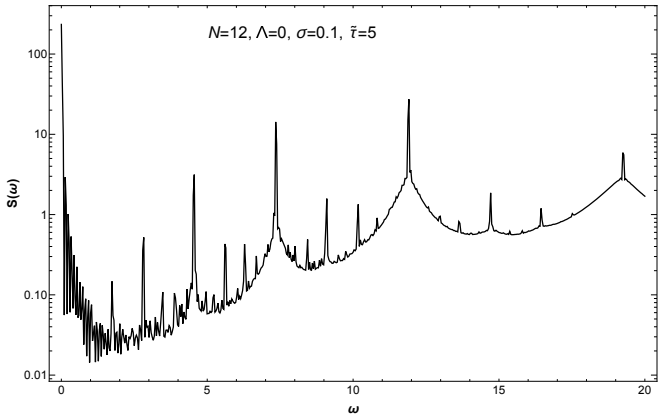

Figure 6. $S(\omega)$ for $N = 12$ for $\sigma = 0.1$ with $\Lambda = 0$ and $\tilde{\tau} = 5$.

4. Conclusions

In this work, we present a theory of the PSD $S(\omega)$ of a Fibonacci signal. In the absence of timing jitter $\xi(t)$, well known results for the PSD $S_0(\omega)$ are obtained. In $S_0(\omega)$, the peaks are intrinsically broadened by the finite generation N of the Fibonacci signal. With increasing N, an increasing number of weak and closely spaced peaks are visually evident in the PSD. In the $N \to \infty$ limit, the PSD is known to be singular-continuous, being composed of a dense set of peaks. We next consider when timing jitter $\xi(t)$ is present to compute $S(\omega)$. Two types of jitter are considered. The first involves a clock that is a self-sustained oscillator, for which the $\xi(t)$ satisfies a one-dimensional diffusion equation [31]. The clock can thus wander over time. This type of jitter results in a PSD $S(\omega)$ in which the spectral peaks are Lorentzian broadened and tend to merge; increasing Λ thus obscures the peaks, with the effect increasing in severity with ω. Minor peaks in $S_0(\omega)$ become entirely indistinct. This type of timing jitter can be fatal to the PSD $S(\omega)$ merging the peaks to the point they are indistinguishable.

The second type of jitter occurs when the clock is subject to a locking oscillator. Here, the jitter is around the absolute time maintained by the locking oscillator, and the jitter obeys a one-dimensional diffusion equation in a harmonic potential [33,38]. Because memory of the absolute time is maintained, the spectral peaks retain a sharp peak at line center, but acquire a pedestal on top of which they sit. The pedestals become higher with increasing ω. Increasing σ or decreasing $\tilde{\tau}$ enhances the relative weight of the pedestals to the line centers. Thus, a locking oscillator can maintain the integrity of the spectrum better than in its absence. It is worth noting that [29] computed purely numerically the effects of a type of disorder in a Fibonacci chain on the spectrum computed based on a tight-binding model similar to this second case of timing jitter and likewise found that the spectrum is robust against this type of disorder. Of course, in practice, the locking oscillator may also be a self-sustaining oscillator (but with very weak diffusion), so both effects may be present. The stochastic model we employ includes the possibility of both effects simultaneously–and to result in closed-form expressions, rahter than to numerically average over many realizations of the timing jitter. In fact, the two different types of timing jitter are temporal analogues of a disorder effect long understood from the theory of x-ray scattering. Our first type of disorder does not conserve long-range temporal order. It is analogous to *type-two disorder*, in the nomenclature of Ref. [39], while our second type of disorder preserves long-range temporal order and is an example of Guinier's *type-one disorder*.

Acknowledgments

DSC gratefully acknowledges the support of Conseil Régional Grand Est.

Conflict of interest

The authors declare no conflict of interest.

References

1. M. Kohmoto, L. P. Kadanoff, C. Tang, Localization problem in one dimension: mapping and escape, *Phys. Rev. Lett.*, **50** (1983), 1870–1872. https://doi.org/10.1103/PhysRevLett.50.1870

2. S. Ostlund, R. Pandit, D. Rand, H. J. Schellnhuber, E. D. Siggia, One-dimensional Schrödinger equation with an almost periodic potential, *Phys. Rev. Lett.*, **50** (1983), 1873–1876. https://doi.org/10.1103/PhysRevLett.50.1873

3. R. Merlin, K. Bajema, R. Clarke, F.-Y. Juang, P. K. Bhattacharya, Quasiperiodic GaAs-A1As heterostructures, *Phys. Rev. Lett.*, **55** (1985), 1768–1770. https://doi.org/10.1103/PhysRevLett.55.1768

4. J. Todd, R. Merlin, R. Clarke, K. M. Mohanty, J. D. Axe, Synchrotron X-ray study of a Fibonacci superlattice, *Phys. Rev. Lett.*, **57** (1986), 1157–1160. https://doi.org/10.1103/PhysRevLett.57.1157

5. M. C. Valsakumar, V. Kumar, Diffraction from a quasi-crystalline chain, *Pramana*, **26** (1986), 215–221. https://doi.org/10.1007/BF02845262

6. D. Paquet, M. C. Joncour, B. Jusserand, F. Laruelle, F. Mollot, B. Etienne, Structural and optical properties of periodic Fibonacci superlattices, In: *Spectroscopy of semiconductor microstructures*, Boston: Springer, 1989, 223–234. https://doi.org/10.1007/978-1-4757-6565-6_14

7. F. Nori, J. P. Rodriguez, Acoustic and electronic properties of one-dimensional quasicrystals, *Phys. Rev. B*, **34** (1986), 2207–2211. https://doi.org/10.1103/PhysRevB.34.2207

8. J. Kollar, A. Sütō, The Kronig-Penney model on a Fibonacci lattice, *Phys. Lett. A*, **117** (1986), 203–209. https://doi.org/10.1016/0375-9601(86)90741-3

9. V. Kumar, G. Ananthakrishna, Electronic structure of a quasiperiodic superlattice, *Phys. Rev. Lett.*, **59** (1987), 1476–1479. https://doi.org/10.1103/PhysRevLett.59.1476

10. J. P. Lu, J. L. Birman, Electronic structure of a quasiperiodic system, *Phys. Rev. B*, **36** (1987), 4471–4474. https://doi.org/10.1103/PhysRevB.36.4471

11. Q. Niu, F. Nori, Renormalization-group study of one-dimensional quasiperiodic systems, *Phys. Rev. Lett.*, **57** (1986), 2057–2060. https://doi.org/10.1103/PhysRevLett.57.2057

12. L. Chen, G. Hu, R. Tao, Dynamical study of a one-dimensional quasi-crystal, *Phys. Lett. A*, **117** (1986), 120–122. https://doi.org/10.1016/0375-9601(86)90016-2

13. M. W. C. Dharma-wardana, A. H. MacDonald, D. J. Lockwood, J.-M. Baribeau, D. C. Houghton, Raman scattering in Fibonacci superlattices, *Phys. Rev. Lett.*, **58** (1987), 1761–1764. https://doi.org/10.1103/PhysRevLett.58.1761

14. M. Nakayama, H. Kato, S. Nakashima, Folded acoustic phonons in (AI, Ga)As quasiperiodic superlattices, *Phys. Rev. B*, **36** (1987), 3472–3474. https://doi.org/10.1103/PhysRevB.36.3472

15. K. Bajema, R. Merlin, Raman scattering by acoustic phonons in Fibonacci GaAs-A1As superlattices, *Phys. Rev. B*, **36** (1987), 4555–4557. https://doi.org/10.1103/PhysRevB.36.4555

16. H. Hiramoto, S. Abe, Anomalous quantum diffusion in quasiperiodic potentials, *Jpn. J. Appl. Phys.*, **26** (1987), 665–666. https://doi.org/10.7567/JJAPS.26S3.665

17. S. Das Sarma, A. Kobayashi, R. E. Prange, Plasmons in aperiodic structures, *Phys. Rev. B*, **34** (1986), 5309–5314. https://doi.org/10.1103/PhysRevB.34.5309

18. P. Hawrylak, J. J. Quinn, Critical plasmons of a quasiperodic semiconductor superlattice, *Phys. Rev. Lett.*, **57** (1986), 380–383. https://doi.org/10.1103/PhysRevLett.57.380

19. M. Goda, Response function and conductance of a Fibonacci lattice, *J. Phys. Soc. Jpn.*, **56** (1987), 1924–1927. https://doi.org/10.1143/JPSJ.56.1924

20. J. B. Sokoloff, Anomalous electrical conduction in quasicrystals and Fibonacci lattices, *Phys. Rev. Lett.*, **58** (1987), 2267–2270. https://doi.org/10.1103/PhysRevLett.58.2267

21. T. Schneider, A. Politi, D. Wiirtz, Resistance and eigenstates in a tight-binding model with quasiperiodic potential, *Z. Phys. B*, **66** (1987), 469–473. https://doi.org/10.1007/BF01303896

22. D. Lusk, I. Abdulhalim, F. Placido, Omnidirectional reflection from Fibonacci quasi-periodic one-dimensional photonic crystal, *Opt. Commun.*, **198** (2001), 273–279. https://doi.org/10.1016/S0030-4018(01)01531-0

23. L. Dal Negro, C. J. Oton, Z. Gaburro, L. Pavesi, P. Johnson, A. Lagendijk, et al., Light transport through the band-edge states of Fibonacci quasicrystals, *Phys. Rev. Lett.*, **90** (2003), 055501. https://doi.org/10.1103/PhysRevLett.90.055501

24. D. Levine, P. J. Steinhardt, Quasicrystals: a new class of ordered structures, *Phys. Rev. Lett.*, **53** (1984), 2477–2480. https://doi.org/10.1103/PhysRevLett.53.2477

25. R. Merlin, Raman studies of Fibonacci, thue-morse, and random superlattices, In: *Light scattering in solids V*, Berlin: Springer, 1989, 214–232. https://doi.org/10.1007/BFb0051990

26. R. Merlin, Structural and electronic properties of nonperiodic superlattices, *IEEE J. Quantum Elect.*, **24** (1988), 1791–1798. https://doi.org/10.1109/3.7108

27. A. Jagannathan, The Fibonacci quasicrystal: case study of hidden dimensions and multifracticality, *Rev. Mod. Phys.*, **93** (2021), 045001. https://doi.org/10.1103/RevModPhys.93.045001

28. R. K. P. Zia, W. J. Dallas, A simple derivation of quasi-crystalline spectra, *J. Phys. A: Math. Gen.*, **18** (1985), L341–L345. https://doi.org/10.1088/0305-4470/18/7/002

29. Y. Liu, R. Riklund, Electronic properties of perfect and non-perfect one-dimensional quasicrystals, *Phys. Rev. B*, **35** (1987), 6034–6042. https://doi.org/10.1103/PhysRevB.35.6034

30. V. Holý, J. Kuběna, K. Ploog, X-ray analysis of structural defects in a semiconductor superlattice, *Phys. Status Solidi. B*, **162** (1990), 347–361. https://doi.org/10.1002/pssb.2221620204

31. M. Lax, Classical noise. V. Noise in self-sustained oscillators, *Phys. Rev.*, **160** (1960), 290–307. https://doi.org/10.1103/PhysRev.160.290

32. R. Adler, A study of locking phenomena in oscillators, *Proceedings of the IRE*, **43** (1946), 351–357. https://doi.org/10.1109/JRPROC.1946.229930

33. H. A. Haus, H. L. Dyckman, Timing of laser pulses produced by combined passive and active mode-locking, *Int. J. Electron.*, **44** (1978), 333–335. https://doi.org/10.1080/00207217808900814

34. A. F. Talla, R. Martinenghi, G. R. Goune Chengui, J. H. Talla Mbé, K. Saleh, A. Coillet, et al., Analysis of phase-locking in narrow-band optoelectronic oscillators with intermediate frequency, *IEEE J. Quantum Elect.*, **51** (2015), 5000108. https://doi.org/10.1109/JQE.2015.2425957

35. S. N. Karmakar, A. Chakrabarti, R. K. Moitra, Dynamic structure factor of a Fibonacci lattice: a renormalization-group approach, *Phys. Rev. B*, **46** (1992), 3660–3663. https://doi.org/10.1103/PhysRevB.46.3660

36. N. Wiener, Generalized harmonic analysis, *Acta Math.*, **55** (1930), 117–258. https://doi.org/10.1007/BF02546511

37. A. Khintchine, Korrelationstheorie der stationären stochastischen Prozesse, *Math. Ann.*, **109** (1934), 604–615. https://doi.org/10.1007/BF01449156

38. D. S. Citrin, Connection between optical frequency combs and microwave frequency combs produced by active-mode-locked lasers subject to timing jitter, *Phys. Rev. Appl.*, **16** (2021), 014004. https://doi.org/10.1103/PhysRevApplied.16.014004

39. A. Guinier, *X-ray diffraction in crystals, imperfect crystals, and amorphous bodies*, San Francisco: W. H. Freeman, 1963.

AIMS Press

© 2023 the Author(s), licensee AIMS Press. This is an open access article distributed under the terms of the Creative Commons Attribution License (http://creativecommons.org/licenses/by/4.0)